China Ocean Eng., 2017, Vol. 31, No. 4, P. 438–446
DOI: 10.1007/s13344-017-0050-1, ISSN 0890-5487
http://www.chinaoceanengin.cn/ E-mail: coe@nhri.cn

Influences of the Helical Strake Cross-Section Shape on Vortex-Induced Vibrations Suppression for A Long Flexible Cylinder

XU Wan-hai[a, b], LUAN Ying-sen[a], LIU Li-qin[a, *], WU Ying-xiang[c]

[a]State Key Laboratory of Hydraulic Engineering Simulation and Safety, Tianjin University, Tianjin 300072, China

[b]Collaborative Innovation Centre for Advanced Ship and Deep-Sea Exploration, Shanghai 200240, China

[c]Institute of Mechanics, Chinese Academy of Sciences, Beijing 100190, China

Received September 2, 2016; revised December 1, 2016; accepted January 18, 2017

Abstract

An experimental study on a bare flexible cylinder as well as cylinders fitted with two types of cross-sectioned helical strakes was carried out in a towing tank. The main purpose of this paper is to investigate the effects of strakes' cross-section on the vortex-induced vibrations (VIV) suppression of a flexible cylinder. The square-sectioned and round-sectioned helical strakes were selected in the experimental tests. The uniform current was generated by towing the cylinder models along the tank using a towing carriage. The Reynolds number was in the range of 800–16000. The strain responses were measured by the strain gages in cross-flow (CF) and in-line (IL) directions. A modal analysis method was adopted to obtain the displacement responses using the strain signals in different measurement positions. The comparison of the experimental results among the bare cylinder, square-sectioned straked cylinder and round-sectioned straked cylinder was performed. The helical strakes can effectively reduce the strain amplitude, displacement amplitude, response frequencies and dominant modes of a flexible cylinder excited by VIV. And the mean drag coefficients of straked cylinders were approximately consistent with each other. In addition, the square-sectioned and round-sectioned strakes nearly share the similar VIV reduction behaviors. Sometimes, the strakes with round-section represent more excellent effects on the VIV suppression of response frequency than those with square-section.

Key words: helical strakes, VIV suppression, cross-section shape, flexible cylinder

Citation: Xu, W. H., Luan, Y. S., Liu, L. Q., Wu, Y. X., 2017. Influences of the helical strake cross-section shape on vortex-induced vibrations suppression for a long flexible cylinder. China Ocean Eng., 31(4): 438–446, doi: 10.1007/s13344-017-0050-1

1 Introduction

Slender marine structures, such as drilling and production risers, tendons and mooring lines, and free spanning pipelines, could be subjected to vortex-induced vibrations (VIV) when exposed to ocean current flows. VIV may cause serious fatigue damageon the structures in offshore engineering. Much research work has been done on this typical fluid-structure interaction phenomenon throughout centuries, both numerically and experimentally, toward the understanding of the dynamic response features of VIV (Naudascher, 1987; Sarpkaya, 2004; Gabbai and Benaroya, 2005; Williamson and Govardhan, 2008; Wu et al., 2012b; Fan et al., 2015) and the VIV suppression (Zdravkovich, 1981; Bearman and Owen, 1998; Galvao et al., 2008; Assi et al., 2009; Wu et al., 2012a; Huera-Huarte, 2014; Gao et al., 2015a, 2015b, 2016).

There are a large number of suppression devices for passively controlling cylinders vibrations undergoing vortex shedding. Among the various geometrical forms of devices for passive VIV suppression, helical strakes are the most common in both air and water, as can be seen in chimneys and subsea tubulars, such as risers, tendons, jumpers, and horizontal pipeline spans (Zdravkovich, 1981). Strakes can not only prevent the shedding from becoming correlated along the span, but also destroy regular vortex shedding. This is why the efficiency of the VIV suppression is very well by means of helical strakes.

The first research work on VIV reduction using helical strakes was carried out by Scruton and Walshe (1957). The helical strakes were subsequently applied to suppress the VIV on cylinders exposed to wind and water. Various geometries of helical strakes, such as strake pitch and strake

Foundation item: This research was supported by the National Natural Science Foundation of China (Grant Nos. 51479135, 51525803 and 51679167), the Science Fund for Creative Research Groups of the National Natural Science Foundation of China (Grant No. 51621092), the Major State Basic Research Development Program of China (973 Program, Grant No. 2014CB046801), and the Natural Science Foundation of Tianjin (Grant No. 15JCQNJC07700).
*Corresponding author. E-mail: liuliqin@tju.edu.cn

height, the number of start screw heads, coverage density, strake cross-section shape, etc., have an obvious effect on VIV suppression.

Many researchers have paid much attention on the optimum configuration of the helical strake pitch and height. Trim et al. (2005) carried out experiments on the VIV suppression of a long flexible cylinder. The geometries of strakes were 17.5D pitch/0.25D height and 5.0D pitch/0.14D height (where D is the cylinder diameter). It was observed that both strake geometries were effective in suppressing the VIV in uniform and shear flow. Quen et al. (2014a) investigated the effectiveness of the strakes for the reduction of VIV of a long flexible cylinder by varying the pitch and height of the strakes. Three configurations of heights (0.05D, 0.10D and 0.15D) and three configurations of pitches (5.0D, 10.0D and 15.0D) were selected in the experimental study. It was found that the larger the strakes' height becomes, the more effective the strakes are in reducing the VIV. Moreover, the influence of the strakes' height is more significant than that of the strakes' pitch in suppressing VIV of a flexible cylinder. Gao et al. (2016) performed some laboratory tests on VIV of a bare cylinder model and straked models with different strakes in a towing tank. The pitches of strakes were 5.0D, 17.5D and 20.0D, and the heights were 0.10D, 0.15D and 0.25D, respectively. It was pointed out that helical strakes with 0.25D/17.5D height/pitch is the best configuration for the VIV suppression of a long flexible cylinder in water. This finding was consistent with the experimental results of Trim et al. (2005).

A few researchers have also studied the effects of the number of start screw heads (Quen et al., 2014b) and strakes coverage density on VIV reduction (Allen et al., 2004; Frank et al., 2004; Trim et al., 2005; Vandiver et al., 2006; Jaiswal and Vandiver, 2007; Gao et al., 2016). Helical strakes generally consist of one or more starts that spiral along the structure's length. If the starts are effectively sized and designed, then the starts cause the vortices to break up into short lengths, and the VIV is efficiently reduced. For cylinders in wind, an effective helical strake geometry has three starts (each spaced 120° apart around the cylinder circumference) (Zhou et al., 2011; Sui et al., 2016). Moreover, it has been proved that the triple-start helical strake system has worked well for many years in water and used popular for VIV suppression of marine slender structures (Trim et al., 2005; Quen et al., 2014a; Gao et al., 2016). In addition, it has also been observed that with the increasing strakes coverage, the VIV suppression efficiency of a flexible cylinder increased gradually to the maximum at 100% coverage (Frank et al., 2004; Trim et al., 2005; Vandiver et al., 2006; Gao et al., 2016).

However, little attention has been paid to the effect of the strake cross-section shape on VIV suppression. Recently, Lubbad et al. (2011) have conducted a series of tests on VIV reduction for an elastically mounted rigid circular cylinder attached with round-sectioned helical strakes. The research work was driven by the fact that round-sectioned helical strakes may represent a very wide and flexible range of use and can be more easily fixed to marine risers compared with sharp-edged strakes. It was found that the optimum configuration for the tested round-sectioned helical strakes suppress the oscillation amplitude relative to the smooth cylinder by 95.6% in CF direction, and by 96.9% in IL direction. To the best knowledge of the authors, the investigation on the VIV suppression for a long flexible cylinder fitted with different types of cross-sectioned strakes is still needed. Therefore, the main aim of this paper is to carry out a series of laboratorytests to investigate the effects of strakes' cross-section on VIV reduction for a flexible cylinder. The bare cylinder model as well as cylinder models attached with square-sectionedandround-sectioned strakes were mounted to a carriage and towed along a towing tank. Parameters of strain, displacement amplitudes, response frequencies and dominant modes as well as hydrodynamic force coefficients are of interest.

The reminder of this paper is organized as follows. In Section 2, the experimental set-up is introduced in detail. The dynamic response characteristics of the bare cylinder as well as the straked cylinder are presented and compared in Section 3. Based on the experimental results, some conclusions are drawn in Section 4.

2 Description of experiment

The experimental investigation mainly concerned on the influences of the cross-section shape of helical strakes on the VIV suppression for a long flexible cylinder. Hence, the most effective configuration of strake with triple-start and 0.25D/17.5D height/pitch for VIV suppression of flexible cylinders in water (Trim et al., 2005; Gao et al., 2015b) was selected in this research work. As shown in Fig. 1, two types of silicone rods with square-section and round-section were used as the helical strakes, which were fitted with the bare flexible cylinder. The bare flexible cylinder with the length of 5.60 m was made of internal copper pipe and outer silicone tube. The inner pipe was a copper tube with an outer diameter of 8.0 mm and a wall thickness of 1.0 mm. The outer pipe was a silicone tube with an outer diameter, D, of 16.0 mm and a wall thickness of 4.0 mm. The aspect ratio (length/diameter, L/D) was equal to 350. The mass per unit length of the cylinder model, m_s was 0.3821 kg/m resulting in the mass ratio $m^*=4m_s/(\rho\pi D^2)$ approximately 1.9 (where ρ is the water density). And the bending stiffness of the model, EI (where E is the Young's modulus and I is the moment of inertia of the copper pipe), was 17.45 N·m^2. Because the outer silicone was soft, its contribution to the bending stiffness can be neglected. The axial tension was directly employed on the inner copper tube. The tension force in the axial direction of the cylinder model, T was 450 N.

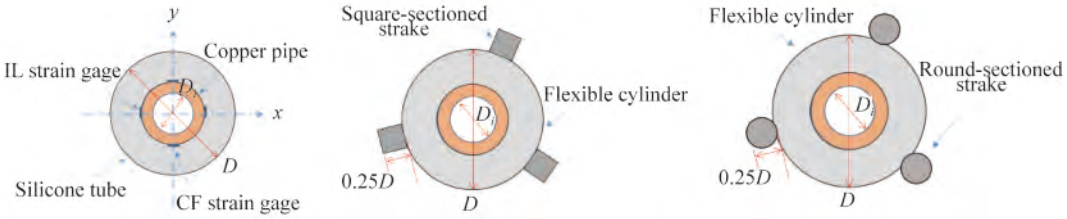

Fig. 1. Cross-section view of the bare cylinder as well as cylinder fitted with square-sectioned and round-sectioned strakes.

The general view of the bare cylinder as well as cylinders fitted with square-sectioned and round-sectioned strakes is shown in Fig. 2. The key parameters in the present experiment are summarized in Table 1. The total of fourteen pairs of strain gages were attached to the outer surface of the copper pipe (see Fig. 1) for obtaining the CF and IL strain signals in seven positions distributed evenly along the cylinder axis. The locations of the pairs of the gages were represented as G1–G7 (see Fig. 3). The sample frequency of strain data was 100 Hz.

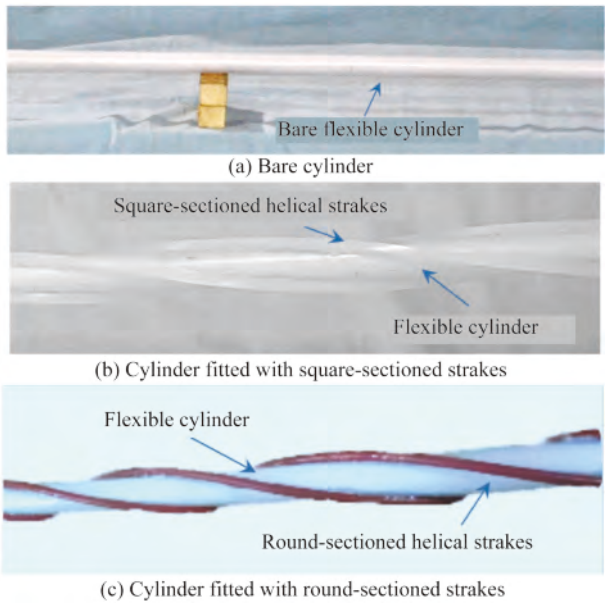

Fig. 2. General view of the cylinder models.

Table 1 Key parameters in the experiment

Parameter	Value
Outer diameter of bare cylinder, D	0.016 m
Total length, L	5.60 m
Bending stiffness, EI	17.45 N·m^2
Axial tension, T	450 N
Mass per unit length of bare cylinder, m_s	0.3821 kg/m
Mass ratio of bare cylinder, m^*	1.90
Aspect ratio of bare cylinder, L/D	350
CF and IL natural frequencies of bare cylinder, f_{CF}, f_{IL}	2.51, 2.53 Hz
Number of starts	3
Strakes pitch/Strakes height	17.5D/0.25D
Towing velocity, U	0.05–1.0 m/s
Reynolds number, Re	800–16000

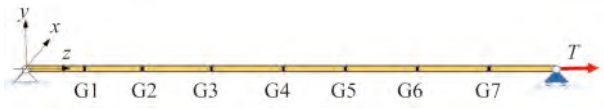

Fig. 3. Locations of strain gages along the cylinder model axis.

The cylinder model was connected to one end of a vertical supporting system using universal joints which can provide pin-pin boundary conditions. The cylinder can bend, but cannot twist in the IL and CF directions. The other end of the vertical supporting system was mounted to a towing carriage in a 137.0 m long, 7.0 m wide and 3.3 m deep towing tank at the State Key Laboratory of Hydraulic Engineering Simulation and Safety, Tianjin University. Experimental schematics are presented in Fig. 4. The bare and straked cylinder models were mounted below the still water level 1.0 m and towed along the tank to simulate the uniform current flow. The towing velocity was in the range of 0.05–1.0 m/s, with the interval of 0.05 m/s. The corresponding Reynolds number ranged from about 800 to 16000.

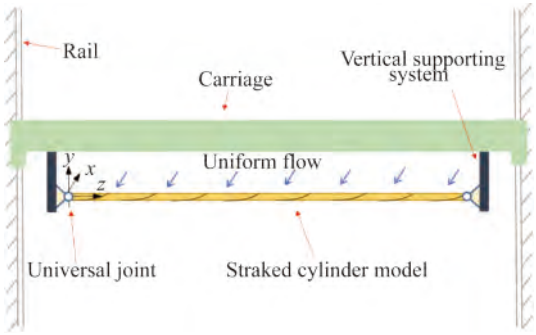

Fig. 4. Experimental schematics.

After the towing carriage velocity was stable, the duration of each test run was 50 s. The waiting time between two consecutive runs was nearly 15 min for eliminating the flow transient effects. A total of 60 runs were carried out across all the cases.

3 Results and discussion

In this section, the reduced velocity is defined as:

$$V_r = \frac{U}{f_1 D}, \tag{1}$$

where U is the towing carriage velocity, and f_1 is the first natural frequency. It can be obtained by experimental test or theoretical calculation. A free decay test in water before performing the experiment was carried out in order to obtain the natural frequencies of the bare cylinder as well as straked cylinders. It can be found that the natural frequencies of bare cylinder were 2.51 Hz and 2.53 Hz in the CF and IL directions, respectively. Because of the slight difference between the first natural frequencies in the CF and IL directions was observed in the free decay test. In this paper, f_1 is calculated by the following equation introduced by Lie and Kaasen (2006) and Song et al. (2011) to simplify the definition of the reduced velocity in the CF and IL directions.

$$f_1 = \frac{1}{2L}\sqrt{\frac{T}{m}+\left(\frac{\pi}{L}\right)^2\frac{EI}{m}}, \tag{2}$$

where m is the unit mass of cylinder model, including the structural mass and the added fluid mass which is defined by $C_a\pi\rho D^2/4$. A modal analysis method was used to obtain the cylinder responses according to the measured bending strain data of the cylinder models (Trim et al., 2005; Lie and Kaasen, 2006; Song et al., 2011; Gao et al., 2016). Firstly, the dynamic response of a bare flexible cylinder excited by the vortex shedding was presented and discussed. Then the effect of the strake's cross-section shape on the VIV suppression was observed and analyzed on the basis of experimental results, including strain responses, displacement amplitudes, dominant response frequencies, dominant modes, and mean drag forces.

3.1 Dynamic characteristics of the bare cylinder

3.1.1 *VIV in CF direction*

The vibrations of the bare cylinder with five carriage towing velocity cases, U=0.1, 0.3, 0.5, 0.7, 0.9 m/s, which were corresponding to the reduced velocities, V_r=2.51, 7.52, 12.53, 17.54, 22.55 respectively, were chosen as some typical examples and investigated in detail.

Fig. 5 shows the spanwise evolutions of dimensionless CF displacement and space-time varying displacement contour in the time range of 20–22 s. The root-mean-square (RMS) CF response amplitude was nearly 0.3D in the case of V_r=2.51. The standing wave or traveling wave was not observed since the lock-in phenomenon did not appear. When the reduced velocity increased to 7.52, the standing wave characteristics were found and the dominant mode was the first, and the maximum response amplitude was about 1.1D. With the increased V_r, it indicated that the VIV response was gradually changing from standing wave behavior to traveling wave behavior (see Figs. 5c–5e). This trend was also found in the experiment on the VIV of a long riser undergoing vortex shedding by Gao et al. (2016). The response amplitude could reach a value of 1.6D with the case of V_r=12.53, and the dominant modes increased from the

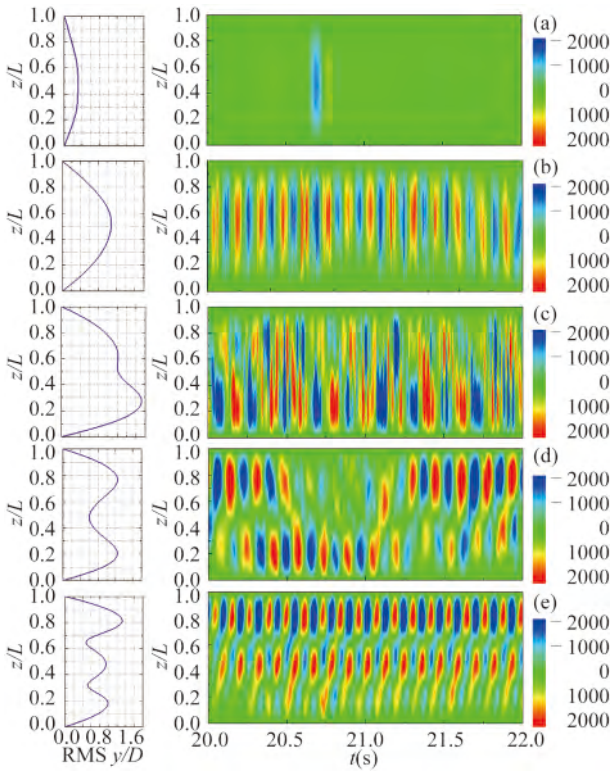

Fig. 5. Spanwise evolutions of the dimensionless CF displacement and space-time varying displacement contour in the time range of 20–22 s with five reduced velocity cases. (a) V_r=2.51; (b) V_r=7.52; (c) V_r=12.53; (d) V_r=17.54; (e) V_r=22.55.

first to the third. In addition, the asymmetry of the spatial distribution of the RMS displacement along the length of the cylinder was also observed, as shown in Figs. 5c and 5e. This could be attributed to the modal composition of the multi-modal VIV with different modal amplitudes, modal frequencies and the phase lags between the excited modes (Song et al., 2011).

For the investigation of the response features in CF direction in detail, the time varying histories of dimensionless CF displacement and response frequencies at the measurement point G4 are presented in Fig. 6. The oscillation frequencies of the bare cylinder were obtained from the displacement response by use of a fast Fourier transform (FFT). When V_r=2.51, the time history of the CF displacement, characterized with a small amplitude, was irregular and periodic. The spectral plot showed a large peak at the frequency of 2.10 Hz and lots of small spikes around, demoting some instability in the vortex shedding (see Fig. 6a).The time varying CF displacement shows a stable curve in the case of V_r=7.52 and 12.53 respectively, as shown in Fig. 6b, and the dominant response frequencies were 2.83 Hz and 4.87 Hz, respectively. In this range of the reduced velocity, the dominant mode swifted from the first mode to the second mode. This was consistent with the results presented in Figs. 5b and 5c. With the reduced velocity in-

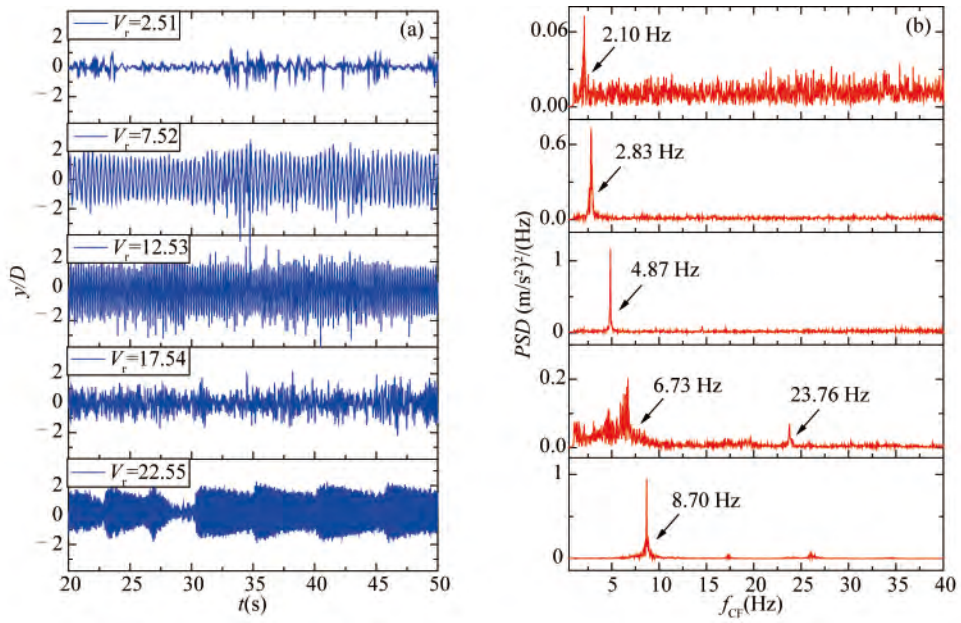

Fig. 6. Time varying histories of the dimensionless CF displacement and response frequencies at the measurement position G4.

creased to a value of 22.55, the displacement response became slightly irregular and the frequencies were dominated with 6.73 Hz and 8.70 Hz, as presented in Fig. 6b. It is clear that the CF VIV responses had one strong frequency peak and a few weak frequency peaks with V_r=17.54. In addition, much higher mode was excited with V_r=22.55.

3.1.2 *VIV in IL direction*

Fig. 7 presents the spanwise evolutions of the dimensionless IL displacement and space-time varying displacement contour. When V_r=2.51, the response amplitude in IL direction was very small and the vibration was obviously weak (see Fig. 7a). When the reduced velocity increased to 7.52, the second mode was excited and the RMS IL displacements associated with the nodes (minima of the response envelope) were close to zero, which clearly represented a standing wave as shown in Fig. 7b. When V_r reached a value of 12.53, the dominant vibration mode was the third and the maximum RMS IL displacement amplitude was larger than 0.4*D* (see Fig. 7c). The overall VIV response was a combination of standing wave and traveling wave behavior; however, it was still dominated by the standing wave. With the increased V_r, the VIV response was gradually changing from standing wave behavior to traveling wave behavior, more details were shown in Figs. 7d and 7e. The maxima of the RMS IL displacement were nearly 0.3*D* and 0.4*D* in the case of V_r=17.54 and 22.55, respectively. And the dominant vibration mode could reach 5.

Fig. 8 gives the time varying histories of the dimensionless IL displacement and response frequencies at the measurement point G4. There was not obvious vibration in IL direction when V_r=2.51. As the value of V_r generally changed from 7.52 to 22.55, the vibration became more and

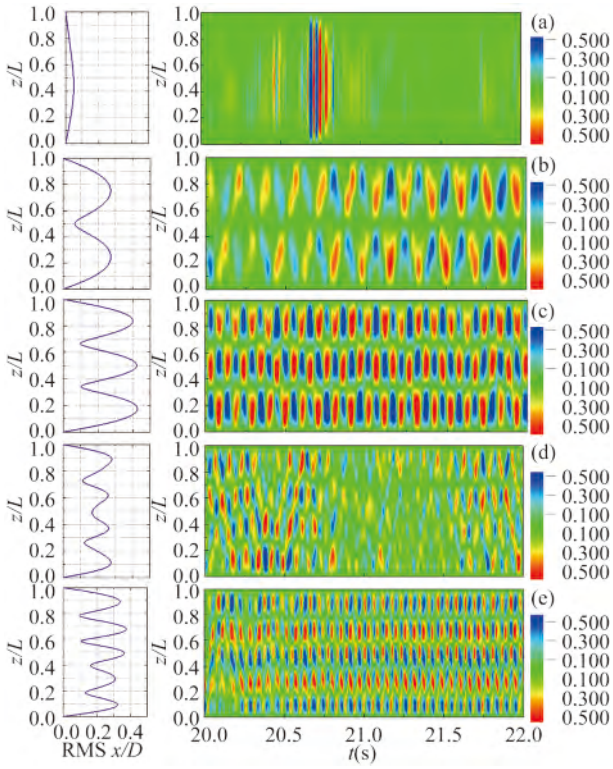

Fig. 7. Spanwise evolutions of the dimensionless IL displacement and space-time varying displacement contour in the time range of 20–22 s with five reduced velocity cases. (a) V_r=2.51; (b) V_r=7.52; (c) V_r=12.53; (d) V_r=17.54; (e)V_r=22.55.

more regular and stable. The lock-in existed in this range of the reduced velocity. Moreover, the dominant response frequencies of the five reduced velocity cases were 2.53 Hz, 8.30 Hz, 9.70 Hz, 11.47 Hz and 17.36 Hz, respectively. Also the higher harmonic phenomenon of IL displacement

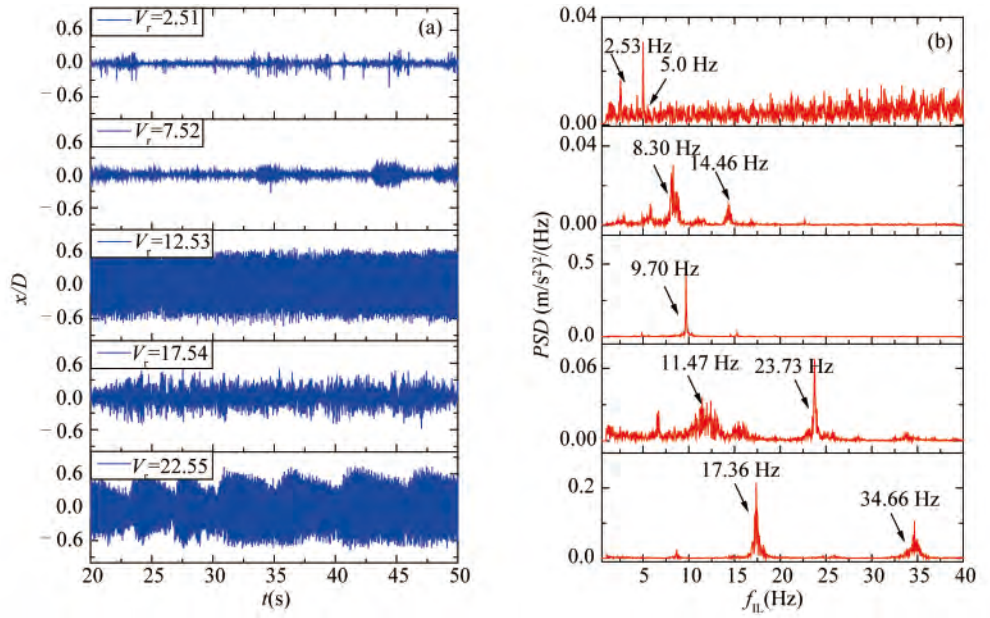

Fig. 8. Time varying histories of the dimensionless IL displacement and response frequencies at the measurement position G4.

response was found in the case of V_r=7.52, 17.54 and 22.55 for a long flexible cylinder excited by VIV.

3.2 Effect of the strake's cross-section shape on VIV suppression

3.2.1 *Strain amplitudes*

The strain was directly measured in the present experiment. It is an important factor for the fatigue damage of structures. Fig. 9 shows the maximum RMS strain amplitudes in the CF and IL directions versus the reduced velocity. The effect of the mean IL deflected shape was removed in the following figures. It indicated that the amplitudes of the CF and IL strains both increased with the reduced velocity for a bare flexible cylinder. Also, it is clear that the strain amplitudes of the bare cylinder due to the IL VIV are similar with magnitude to those produced by vortex shedding in CF direction. The CF and IL strain responses were both obviously reduced by attaching helical strakes with square-section and round-section. The CF strain amplitude of the straked cylinder was really small. The maximum RMS strain amplitudes of the round-sectioned straked cylinder were 20.0 and 8.0 με in the CF and IL directions, respectively. It also can be found that the square-sectioned straked cylinder and round-sectioned straked cylinder shared similar strain amplitude behaviors versus the reduced velocity. It means that the round-sectioned strakes could reduce strain response as well as square-sectioned ones.

3.2.2 *Displacement amplitudes*

As illustrated in Fig. 10, the maximum RMS dimensionless displacement in the CF and IL directions versus the reduced velocity is plotted. It can be clearly seen that the CF

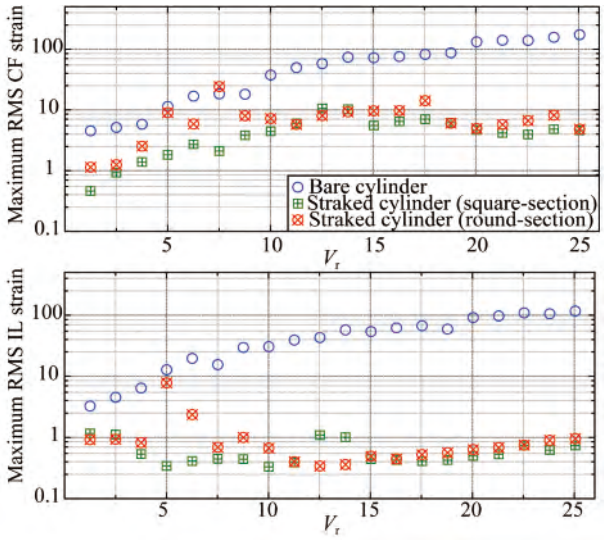

Fig. 9. Maximum RMS strain amplitude vs. the reduced velocity.

response amplitudes of the bare cylinder could be up to a value of 1.6*D* and the IL ones more than 0.4*D*. It is shown that there was a sudden drop both in the CF and IL directions and the reduced velocity corresponding to the drop wasin the range of 6.6 to 9.5. The mode transition occurred in this region and the response amplitude decreased in the mode transition region. It was observed that the CF displacement of a bare cylinder was generally approximately two to four times that in the IL direction, but they were still in the same order. For the straked cylinder with square-section and round-section, the VIV response of the flexible cylinder with the strake configurations of 17.5*D*/0.25*D* was suppressed significantly. It means that the influences of the cross-sectioned strake on the VIV reduction were not obvi-

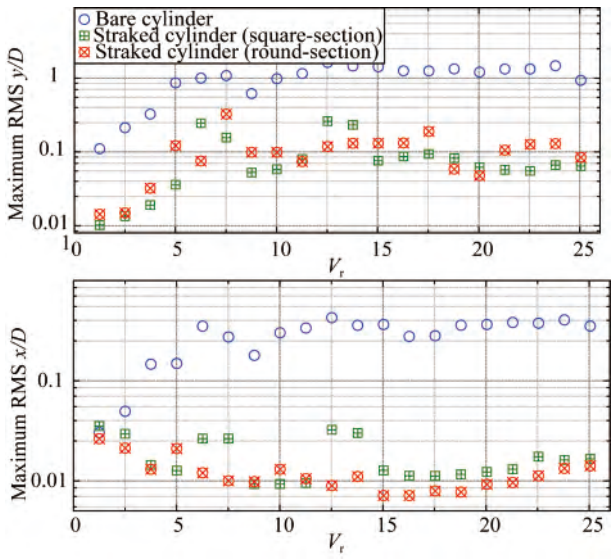

Fig. 10. Maximum RMS dimensionless displacement vs. the reduced velocity.

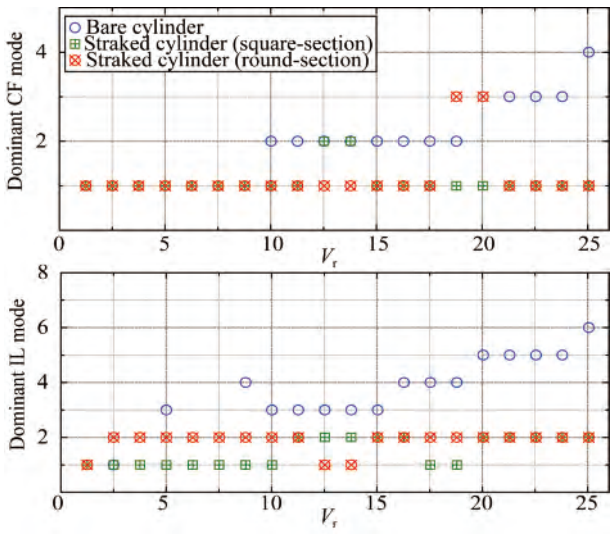

Fig. 12. Dominant modes vs. the reduced velocity.

ous. In addition, the response amplitude suppression efficiencies of the straked cylinder with different cross-section shapes versus the reduced velocity are presented in Fig. 11. Herein, the suppression efficiency of response amplitude, is defined as $\eta = [(Bare - Straked)/Bare] \times 100\%$ (*Bare* is the dimensionless RMS amplitude of the flexible bare cylinder in CF or IL direction and *Straked* is that of the flexibly straked cylinder at the same reduced velocity) is used to investigate the decrease of the maximum value of RMS displacement. It can be found that the VIV suppression efficiency in this research work was similar with the experimental results of Trim et al. (2005). It is also proved that the suppression efficiency was nearly the same even though the cross-sections are square and round, respectively.

3.2.3 *Dominant response frequencies and dominant modes*

The dominant mode numbers in the CF and IL directions against the reduced velocity are given in Fig. 12. It can be found that the dominant modes of the bare cylinder increased gradually with the increase of the reduced velocity. The CF dominant modes were up to the fourth while the IL the sixth. As discussed by a few researchers (Chaplin et al., 2005; Lie and Kaasen, 2006), the overall response of a long flexible cylinder generally combines not only one excited mode over a certain range of the reduced velocity. Thus, the dominant modes investigated here are not always the highest one as the reduced velocity increases.The maximum CF and IL dominant modes for the square-sectioned straked cylinder were both Mode 2, which were lower than that for the bare cylinder. Meanwhile, the maximum dominant modes for the round-sectioned straked cylinder were Mode 3 in the CF direction and Mode 2 in the IL direction. It suggests that the dominant modes for the straked cylinder were significantly reduced by the helical strakes with different cross-sections.

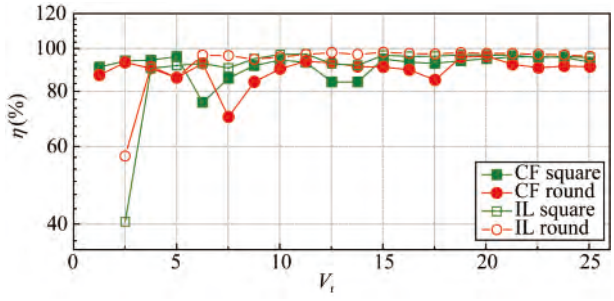

Fig. 11. Response amplitude suppression efficiencies of the straked cylinder with different cross-section shapes vs. the reduced velocity.

The dominant frequencies of the bare cylinder as well as the straked cylinders are drawn in Fig. 13. It appears that the variation of the dominant frequencies of the bare cylinder increased linearly with the reduced velocity. A linear fit with a slope of 0.171 could be obtained in the figure of the CF dominant frequencies. Also it should be pointed out that the IL dominant frequency was nearly twice that in the CF direction. This trend is consistent with the dominant mode trends in Fig. 12. However, the dominant frequency of the flexible cylinder fitted with helical strakes did not increase linearly with the reduced velocity anymore. This trend is similar to the experimental results of the VIV suppression by several previous researchers (Trim et al., 2005; Quen et al., 2014a; Gao et al., 2015b). In addition, the frequency reduction with the round-sectioned strakes was more effective than that of the square-sectioned strakes, especially in the CF direction.

3.2.4 *Mean drag forces*

The mean drag coefficients C_d of cylinder models, including the bare cylinder and straked cylinders, are illustrated in Fig. 14. In order to compare with other experiments, the results from Quen et al. (2014a) of the flexible

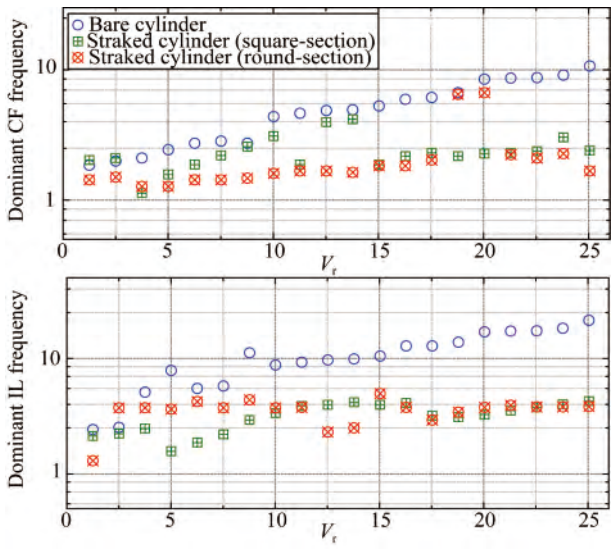

Fig. 13. Dominant frequencies vs. the reduced velocity.

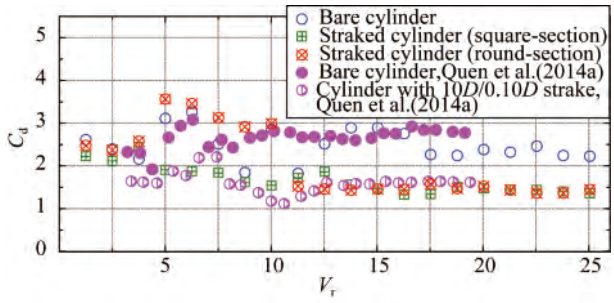

Fig. 14. Mean drag force coefficients vs. the reduced velocity.

cylinder are also shown in Fig. 14. The average C_d of the bare cylinder in the present tests throughout the entire reduced velocity range was approximately 2.49, which was nearly same with the value of Quen et al. (2014a). When the bare cylinder was attached with round-sectioned strakes, the mean drag coefficients generally increased to a value of 3.5 and then drop slightly with V_r as up to 10.0, and then the mean drag coefficients were smaller than those of the bare cylinder. However, the mean drag coefficients of the square-sectioned straked cylinder were not larger than the results of the bare cylinder. This phenomenon was also observed in the experiment of the VIV reduction for a flexible cylinder (Quen et al., 2014a). The mean drag coefficients of the straked cylinders present a scattered feature as those of Huera-Huarte and Bearman (2009) and Gu et al. (2013) on the bare flexible cylinder. In addition, the mean drag coefficients of the flexible cylinder fitted with the round-sectioned strakes were similar with those of square-sectioned straked cylinder, except for that the reduced velocity was in the range of 5.0–10.0.

4 Conclusions

The VIV reduction of a flexible cylinder fitted with two types of cross-sectioned strakes (square-section and round-section) were experimentally investigated in the towing tank. To examine the influences of the strake cross-section on the VIV suppression, the dynamic features of the bare cylinder and straked cylinders, including the strain response, displacement amplitudes, dominant response frequencies, dominant modes, and mean drag force coefficients were analyzed and discussed. The following conclusions can be drawn.

(1) For the bare flexible cylinder, the maximum RMS CF response amplitude could reach a value of 1.6*D* and the IL more than 0.4*D*. The overall VIV response was a combination of standing wave and traveling wave behavior with the reduced velocity increased to a large value. Meanwhile, the asymmetry of the spatial distribution of the RMS displacement along the length of the cylinder was observed, and the higher harmonic phenomenon of the displacement response was also found. The average value of the mean drag coefficients was approximately 2.49 in the present experiment. These findings were consistent with previous VIV experimental results of bare flexible cylinders (Trim et al., 2005; Song et al., 2011; Quen et al., 2014a; Gao et al., 2016).

(2) For the flexible cylinder fitted with square-sectioned strakes, the strain, response displacement, dominant frequencies and modes were apparently reduced. It was experimentally proved that the strake with triple-start and 0.25*D*/17.5*D* height/pitch is the most effective configuration for the VIV reduction of the flexible cylinders in water. The similar findings were also presented by Trim et al. (2005) and Gao et al. (2015b).

(3) For the flexible cylinder fitted with round-sectioned strakes, the suppression of strain responses and displacement amplitudes was as good as that of the cylinder attached with square-sectioned strakes. In addition, the frequency reduction was more effective than that of the square-sectioned strakes, especially in the CF direction. The mean drag coefficient was much larger when the reduced velocity was in the range of 5.0–10.0. And the mean drag coefficients of the straked cylinders were in good agreement with each other.

References

Allen, D.W., Henning, D.L. and Lee, L.W., 2004. Performance comparisons of helical strakes for VIV suppression of risers and tendons, *Proceedings of the Offshore Technology Conference*, Offshore Technology Conference, Houston, TX, OTC16186.

Assi, G.R.S., Bearman, P.W. and Kietney, N., 2009. Low drag solutions for suppressing vortex-induced vibration of circular cylinders, *Journal of Fluids and Structures*, 25(4), 666–675.

Bearman, P.W. and Owen, J.C., 1998. Reduction of bluff-body drag and suppression of vortex shedding by the introduction of wavy separation lines, *Journal of Fluids and Structures*, 12(1), 123–130.

Chaplin, J.R., Bearman, P.W., HueraHuarte, F.J. and Pattenden, R.J., 2005. Laboratory measurements of vortex-induced vibrations of a

vertical tension riser in a stepped current, *Journal of Fluids and Structures*, 21(1), 3–24.

Fan, Y.T., Mao, H.Y., Guo, H.Y., Liu, Q.H. and Li, X.M., 2015. Experimental investigation on vortex-induced vibration of steel catenary riser, *China Ocean Engineering*, 29(5), 691–704.

Frank, W.R., Tognarelli, M.A., Slocum, S.T., Campbell, R.B. and Balasubramanian, S., 2004. Flow-induced vibration of a long, flexible, straked cylinder in uniform and linearly sheared currents, *Proceedings of the Offshore Technology Conference*, Offshore Technology Conference, Houston, TX, OTC16340.

Gabbai, R.D. and Benaroya, H., 2005. An overview of modeling and experiments of vortex-induced vibration of circular cylinders, *Journal of Sound and Vibration*, 282(3–5), 575–616.

Galvao, R., Lee, E., Farrell, D., Hover, F., Triantafyllou, M., Kitney, N. and Beynet, P., 2008. Flow control in flow-structure interaction, *Journal of Fluids and Structures*, 24(8), 1216–1226.

Gao, Y., Fu, S.X., Cao, J. and Chen, Y.F., 2015a. Experimental study on response performance of VIV of a flexible riser with helical strakes, *China Ocean Engineering*, 29(5), 673–690.

Gao, Y., Fu, S.X., Ren, T., Xiong, Y.M. and Song, L.J., 2015b. VIV response of a long flexible riser fitted with strakes in uniform and linearly sheared currents, *Applied Ocean Research*, 52, 102–114.

Gao, Y., Yang, J.D., Xiong, Y.M., Wang, M.H. and Peng, G., 2016. Experimental investigation of the effects of the coverage of helical strakes on the vortex-induced vibration response of a flexible riser, *Applied Ocean Research*, 59, 53–64.

Gu, J.J., Vitola, M., Coelho, J., Pinto, W., Duan, M.L. and Levi, C., 2013. An experimental investigation by towing tank on VIV of a long flexible cylinder for deepwater riser application, *Journal of Marine Science and Technology*, 18(3), 358–369.

Huera-Huarte, F.J., 2014. On splitter plate coverage for suppression of vortex-induced vibrations of flexible cylinders, *Applied Ocean Research*, 48, 244–249.

Huera-Huarte, F.J. and Bearman, P.W., 2009. Wake structures and vortex-induced vibrations of a long flexible cylinder–Part 2: drag coefficients and vortex modes, *Journal of Fluids and Structures*, 25(6), 991–1006.

Jaiswal, V. and Vandiver, J.K., 2007. VIV response prediction for long risers with variable damping, *Proceedings of the 26th International Conference on Offshore Mechanics and Arctic Engineering*, ASME, San Diego, CA, USA, OMAE2007–29353.

Lie, H. and Kaasen, K.E., 2006. Modal analysis of measurements from a large-scale VIV model test of a riser in linearly sheared flow, *Journal of Fluids and Structures*, 22(4), 557–575.

Lubbad, R.K., Løset, S. and Moe, G., 2011. Experimental investigations of the efficiency of round-sectioned helical strakes in suppressing vortex induced vibrations, *Journal of Offshore Mechanics and Arctic Engineering*, 133, 041102.

Naudascher, E., 1987. Flow-induced streamwise vibrations of structures, *Journal of Fluids and Structures*, 1(3), 265–298.

Quen, L.K., Abu, A., Kato, N., Muhamad, P., Sahekhaini, A. and Abdullah, H., 2014a. Investigation on the effectiveness of helical strakes in suppressing VIV of flexible riser, *Applied Ocean Research*, 44, 82–91.

Quen, L.K., Abu, A., Muhamad, P., Kato, N., Sahekhaini, A. and Abdullah, H., 2014b. The effectiveness of two- versus three-start helical strakes in suppressing VIV of flexible cylinder, *Proceedings of the Offshore Technology Conference-Asia*, Offshore Technology Conference, Kuala Lumpur, Malaysia.

Sarpkaya, T., 2004. A critical review of the intrinsic nature of vortex-induced vibrations, *Journal of Fluids and Structures*, 19(4), 389–447.

Scruton, C. and Walshe, D.E.J., 1957. *A Means for Avoiding Wind-Excited Oscillations of Structures with Circular or Nearly Circular Cross-Section*, National Physics Laboratory Report NPL/Aero/335, National Physics Laboratory, Great Britain.

Song, J.N., Lu, L., Teng, B., Park, H.I., Tang, G.Q. and Wu, H., 2011. Laboratory tests of vortex-induced vibrations of a long flexible riser pipe subjected to uniform flow, *Ocean Engineering*, 38(11–12), 1308–1322.

Sui, J., Wang, J.S., Liang, S.P. and Tian, Q.L., 2016. VIV suppression for a large mass-damping cylinder attached with helical strakes, *Journal of Fluids and Structures*, 62, 125–146.

Trim, A.D., Braaten, H., Lie, H. and Tognarelli, M.A., 2005. Experimental investigation of vortex-induced vibration of long marine risers, *Journal of Fluids and Structures*, 21(3), 335–361.

Vandiver, J.K., Swithenbank, S., Jaiswal, V. and Marcollo, H., 2006. The effectiveness of helical strakes in the suppression of high-mode-number VIV, *Proceedings of the Offshore Technology Conference*, Offshore Technology Conference, Houston, TX, OTC18276.

Williamson, C.H.K. and Govardhan, R., 2008. A brief review of recent results in vortex-induced vibrations, *Journal of Wind Engineering and Industrial Aerodynamics*, 96(6–7), 713–735.

Wu, H., Sun, D.P., Lu, L., Teng, B., Tang, G.Q. and Song, J.N., 2012a. Experimental investigation on the suppression of vortex-induced vibration of long flexible riser by multiple control rods, *Journal of Fluids and Structures*, 30, 115–132.

Wu, X.D., Ge, F. and Hong, Y.S., 2012b. A review of recent studies on vortex-induced vibrations of long slender cylinders, *Journal of Fluids and Structures*, 28, 292–308.

Zdravkovich, M.M., 1981. Review and classification of various aerodynamic and hydrodynamic means for suppressing vortex shedding, *Journal of Wind Engineering and Industrial Aerodynamics*, 7(2), 145–189.

Zhou, T., Razali, S.F.M., Hao, Z. and Cheng, L., 2011. On the study of vortex-induced vibration of a cylinder with helical strakes, *Journal of Fluids and Structures*, 27(7), 903–917.